Supplementary Material

1D Rod-like {220}-faceted CeO_2/ZnO S-scheme heterojunctions: Design, Photocatalytic Mechanism and DFT calculations

Qiang Wang[1], Chao Yao[1], Xin Liu[1], Junfeng Qiu[1], Rongchen Wang[1], Jialong Liu[1*], Wei Wang[1, 2*]

[1] Department of Physics and Electronics, School of Mathematics and Physics, Beijing University of Chemical Technology, Beijing 100029, China

[2] Beijing Key Laboratory of Environmentally Harmful Chemical Analysis, Beijing University of Chemical Technology, Beijing 100029, China

[*] Corresponding authors. E-mail: jialongliu@buct.edu.cn (Jialong Liu); wangwei@mail.buct.edu.cn (Wei Wang).

S1. Specific instrument models and operating parameters.

X-ray diffraction (XRD, Rigaku D/max X-ray diffractometer, Cu Kα), scanning electron microscopy (SEM, Hitachi S4700), and transmission electron microscopy (TEM, FEI Tecnai G2) equipped with energy dispersive spectroscopy were used to analyzed the crystal structure, morphology, composition and elemental mapping of the as-prepared samples. X-ray photoelectron spectroscopy (XPS) was performed on a VG ESCALAB 220 IXL photoelectron spectrometer employing Al Kα radiation (10 KeV/150 W) and a concentric hemi-spherical electron energy analyzer with a passing energy of 40 eV. The as-prepared sample was uniformly pressed onto the carbon tape attached on the sample stub, after which the stub was gently shaken to remove excess powder before transferring into the vacuum chamber. The analysis chamber was operating at a vacuum of 5×10^{-9} mbar. The surface area was obtained by the Brunauer-Emmett-Teller (BET) technique using an automatic specific surface and porosity analyzer (Micromeritics ASAP 2460). The optical performance was characterized by UV–vis diffusive reflectance spectra on a spectrophotometer (Shimadzu, UV-2501PC) and photoluminescence (PL) spectra (Hitachi F-7000 Fluorescence Spectrophotometer). A total organic carbon analyzer (TOC-L) was applied to evaluate the mineralization of the TC solution. Electron spin resonance spectroscopy (ESR, Elexsys-II E500) was used to detect the $\cdot O_2^-$ and ·OH signals. The intermediate products generated in the TC degradation processes were measured by the LC-MS (Waters ACQUITY UPLC XEVO-G2 QTOF).

S2. Photoelectrochemical activity

An electrochemical workstation (CHI660E) with three-electrode system was used to measure the photoelectrochemical activity of the samples. Here, Ag/AgCl electrode and Pt plate (1 × 1 cm^2) were the reference electrode and the counter electrode, respectively. Next, as to the preparation of the working electrode, 10 mg of the sample was dispersed in a mixed ink (100 μL water/50 μL ethanol/50 μL Nafion), and the mixed solutions were sonicated for 10 min. Further, the mixed ink was dropped onto an FTO glass (1 × 2 cm^2) and dried for 12 h. The Na_2SO_4 solution (0.5 M, pH = 6.1) was used as the electrolyte. The same xenon lamp was also used to provide light for the working electrode. In the frequency range of 0.01–100000 Hz, the electrochemical impedance spectra (EIS) were measured. The flat-band potentials were tested using the Mott-Schottky (MS) method at 1500 Hz.

S3. Relevant parameters for DFT calculations.

The cut-off energy of the plane wave basis was set to 750 eV. The convergence tolerance parameter for the max step size was 0.001 Å. The maximum force was 0.03 eV/Å. The energy change was 1.0×10^{-5} eV/atom and maximum stress was 0.05 GPa. Also, 3 × 3 × 1 Monkhorst-Pack lattice sampling of the K points in the first Brillouin zone was performed for self-consistent calculations.

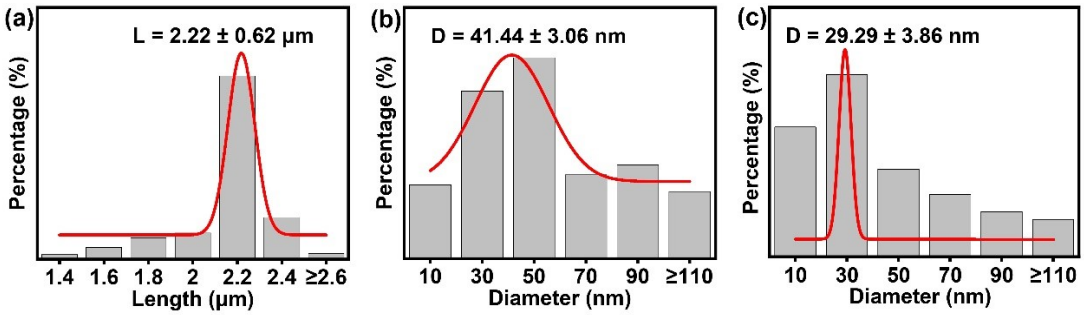

Fig. S1. (a) Length distribution of CeO_2 nanorods. Size distribution of ZnO nanoparticles in (b) pristine ZnO and (c) CZ-2.

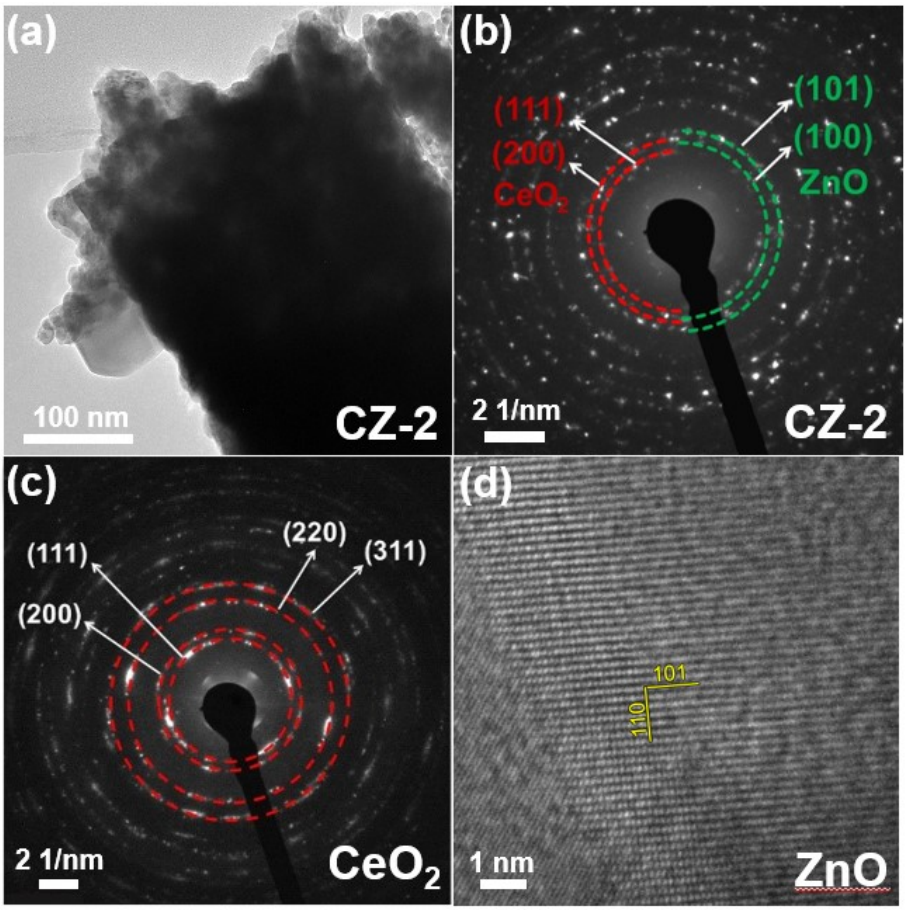

Fig. S2. (a) TEM image and (b) SAED patterns of CZ-2 composite. (c) SAED patterns of CeO_2. (d) HRTEM image of ZnO.

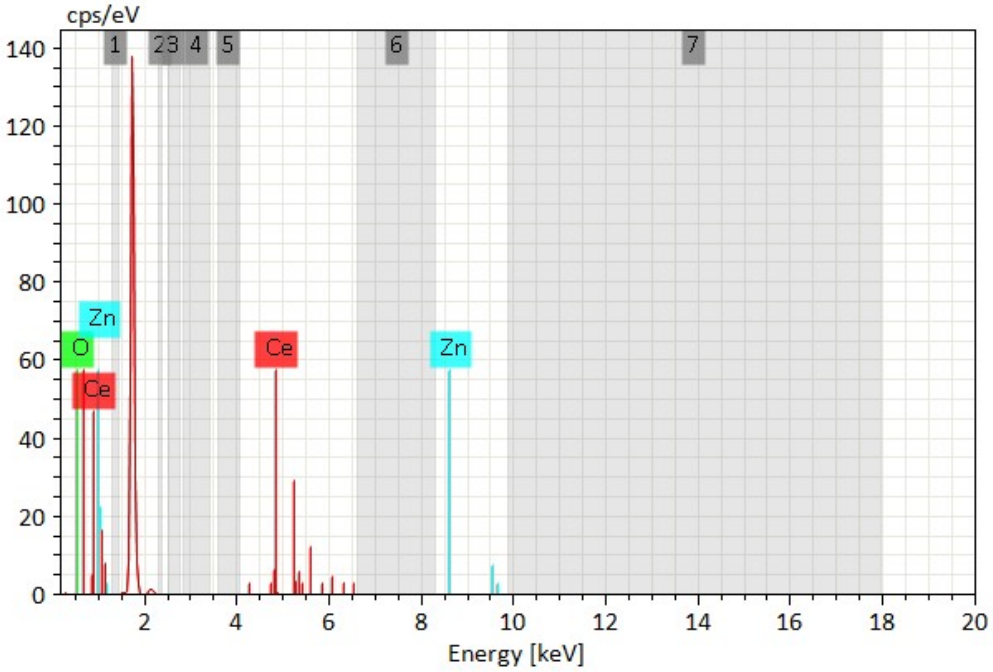

Elements	Atomic number	Mass [%]	Atom [%]
O	8	10.13	43.29
Zn	30	23.07	24.12
Ce	58	66.80	32.59
		100.00	100.00

Fig. S3. EDS spectrum and element composition of CZ-2.

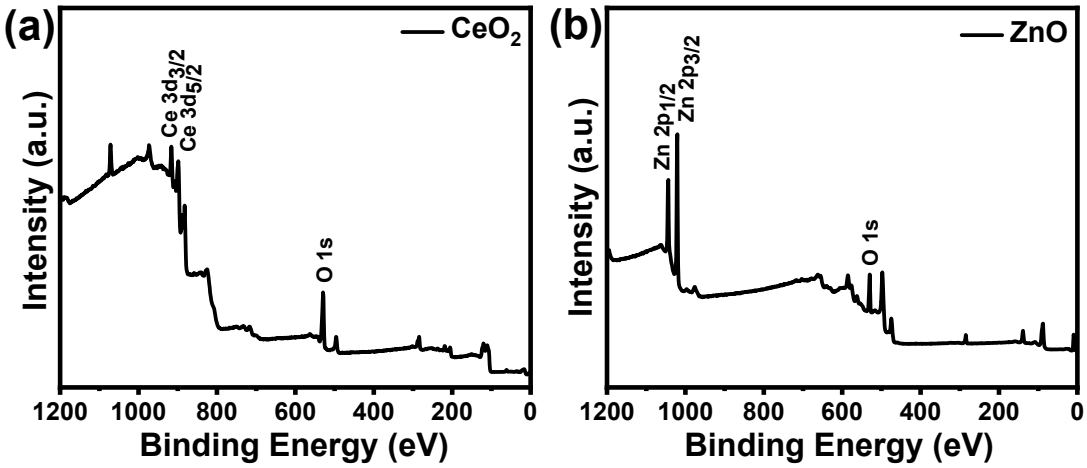

Fig. S4. XPS spectra of (a) CeO_2, (b) ZnO.

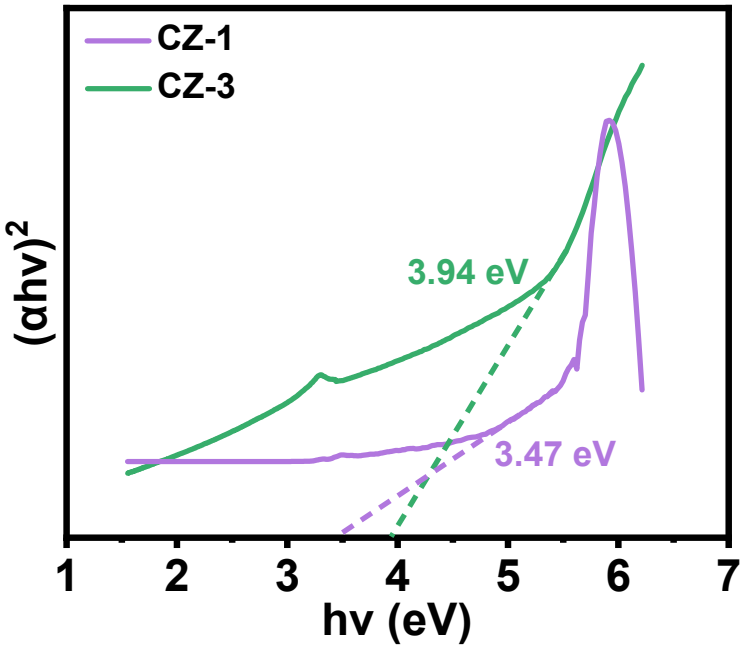

Fig. S5. Fitted band gaps of CZ-1 and CZ-3.

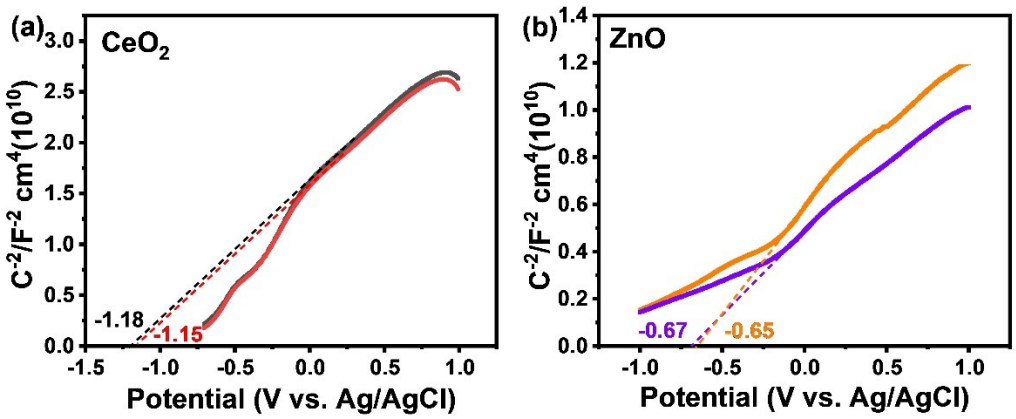

Fig. S6. Mott–Schottky plots for repeated experiments of (a) CeO_2 and (b) ZnO.

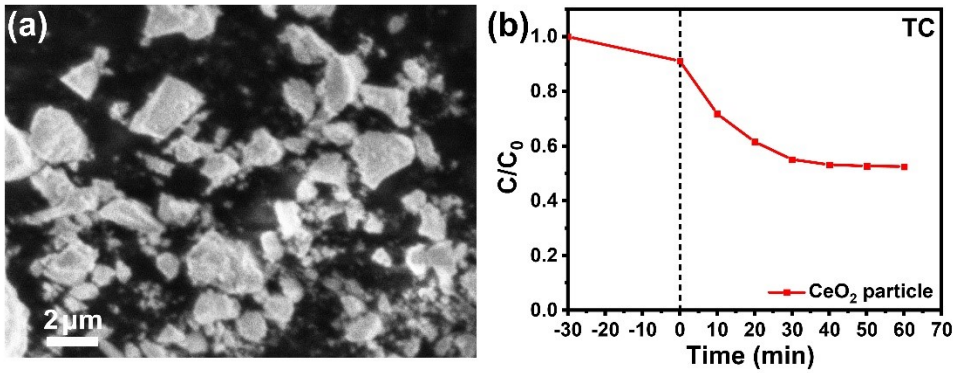

Fig. S7. (a) SEM images of CeO_2 particles. (b) Photocatalytic removal curve of TC for CeO_2 particles.

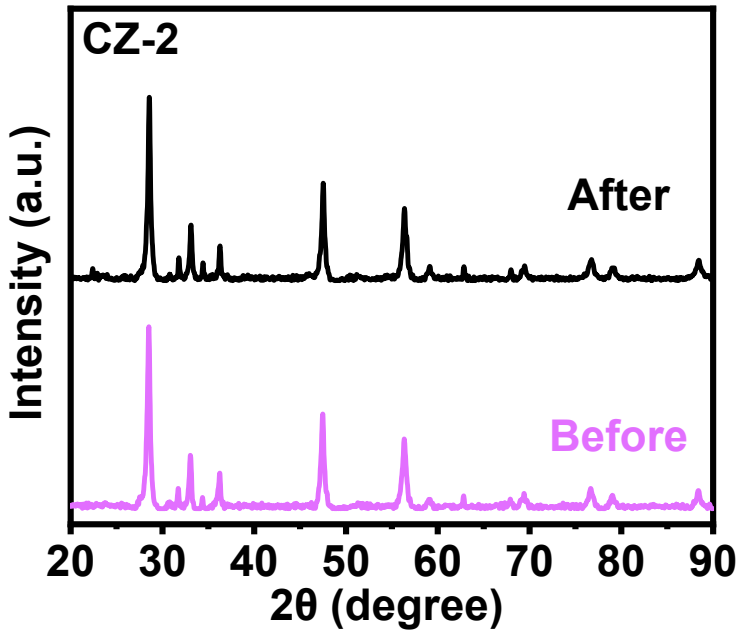

Fig. S8. XRD patterns of original CZ-2 and the collected sample after cyclic experiment of TC.

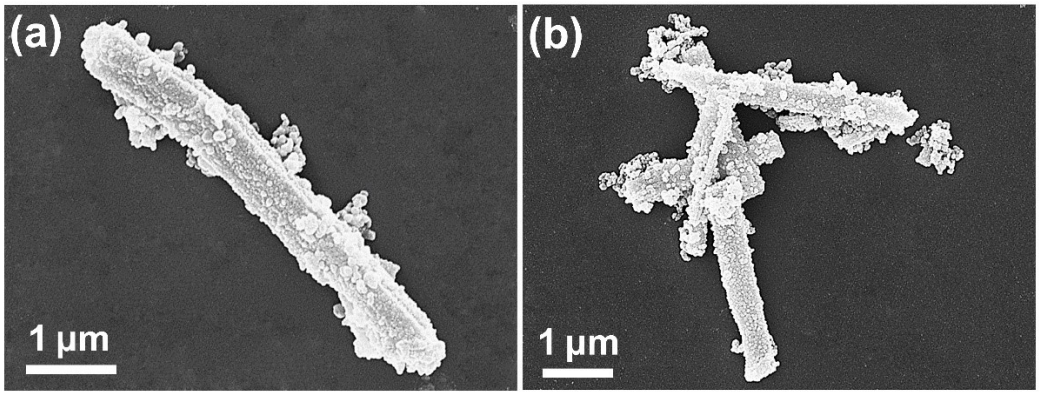

Fig. S9. The SEM images of CZ-2 after the photodegradation experiment.

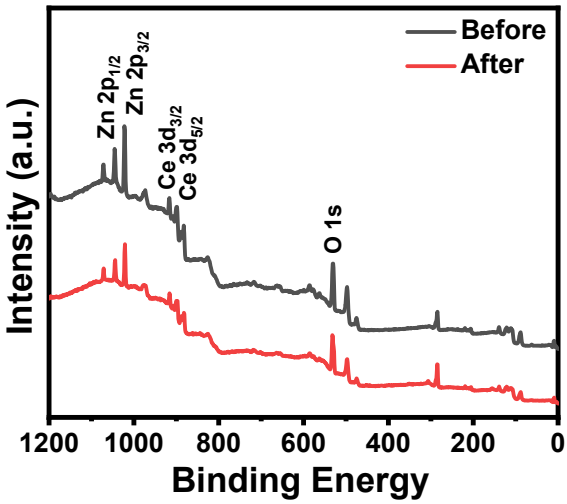

Fig. S10. The XPS spectra of CZ-2 before and after the photodegradation experiment.

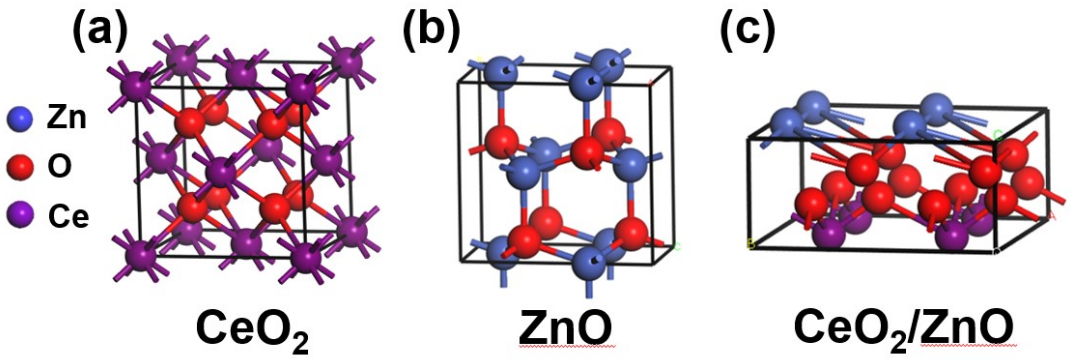

Fig. S11. The optimized geometric structures of (a) CeO_2, (b) ZnO and (c) CeO_2/ZnO.

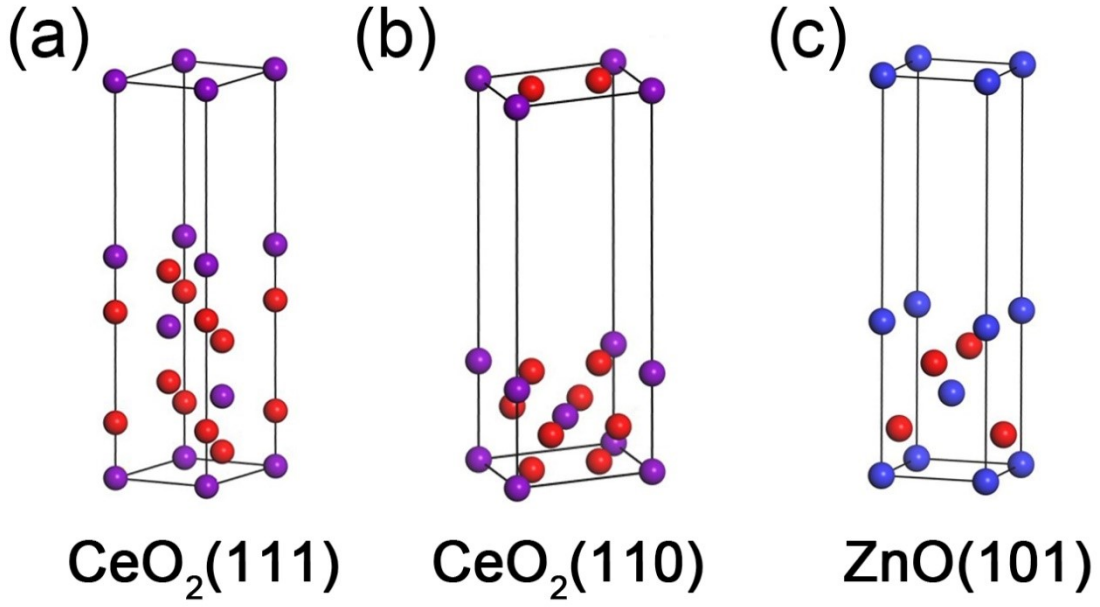

Fig. S12. The crystal structure and the optimized geometric structures of (a) $CeO_2(111)$, (b) $CeO_2(110)$ and (c) ZnO(101).

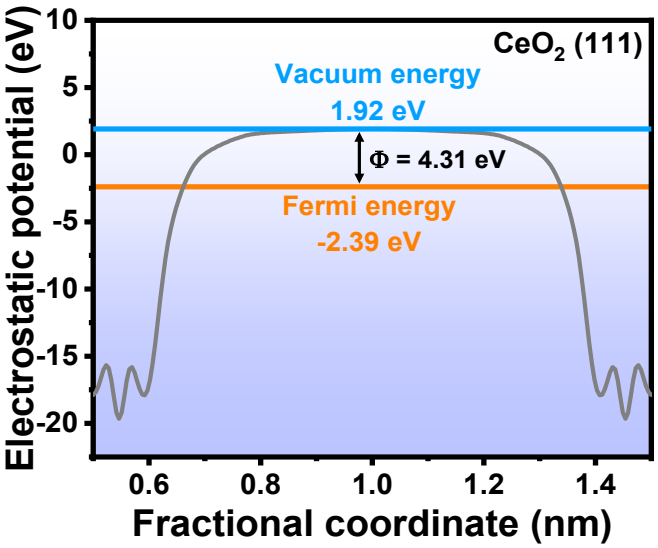

Fig. S13. The work function of CeO_2(111).

Table S1. BET (S_{BET}), pore sizes (D_p) and pore volume (V_p) of CeO_2, ZnO and CZ-2.

Sample	S_{BET} (m^2 g^{-1})	D_p (nm)	V_p (cm^3 g^{-1})
CeO_2	10.40	36.14	0.09
ZnO	17.62	47.69	0.21
CZ-2	28.62	10.75	0.08

Table S2. Flat-band potentials of CeO_2 and ZnO.

Number of tests / Flat-band potentials (eV)	1	2	3	Average
CeO_2	-1.17	-1.18	-1.15	-1.17
ZnO	-0.66	-0.67	-0.65	-0.66